JOURNAL OF CATALYSIS 84, 256–260 (1983)

Characterization of X-Ray Amorphous ZSM-5 Zeolites by High Resolution Solid State ^{13}C-NMR Spectroscopy

The unique molecular shape-selective properties of ZSM-5 type zeolites in catalytic reactions, which are due to the particular structure of these materials (*1–3*), can be affected by different factors, such as steric modifications of their channel system by various chemicals (*4–8*) or controlled surface coking (*7–9*). The effect of size and shape of the zeolite particles was also considered (*10, 11*). The control of these parameters results in materials showing more uniform shape-selective properties which are desired for various industrial applications (*10*).

We have recently developed several synthesis procedures, yielding ZSM-5 materials differing in size, homogeneity, morphology, and composition (*12*). Various experimental factors influencing these properties have been thoroughly discussed (*13*). In particular, we have shown that under specific synthesis conditions, very small ZSM-5 particles are obtained from the aluminosilicate hydrogel precursor and are stabilized in the early stages of the crystallization process. Although they are still too small to be detected by the X-ray diffraction method (*12, 14, 15*), infrared spectra confirmed the presence of ZSM-5 agglomerates of less than 8 nm in size, embedded within an amorphous matrix (*14, 16*). Furthermore, such materials were shown to exhibit shape-selective properties in hydroconversion of long-chain paraffins (*14*).

Another way to characterize quantitatively these X-ray amorphous particles is to detect the presence of strongly bound structure-directing organic guest molecules or ions, such as tetrapropylammonium (TPA) ions, occluded within the zeolitic framework, but absent in the amorphous gel phase. The amount of TPA, which is then proportional to the percentage of crystalline ZSM-5 present in the phase, could be determined by thermal analysis, either by measuring the weight loss corresponding to the oxidative decomposition and release of TPA ions between 300 and 600°C (*12*), or by determining the surface area of the corresponding DTA peak (*15*).

Recently, high resolution magic-angle-spinning (HRMAS) ^{13}C-NMR spectroscopy was successfully used to characterize the position and configuration of various guest organic molecules, among them TPA, occluded in the framework of 100% crystalline ZSM-5 particles (*17–19*).

In the present work, we wish to show the ability of that technique to probe the presence of TPA entities in small X-ray amorphous ZSM-5 particles and to illustrate its potential use in following quantitatively the progressive growth of ZSM-5 crystallites. Two different crystallization procedures were chosen as comparative examples. In procedure A, a small number of X-ray detectable ZSM-5 crystallites are already formed in solution in the early stage of the crystallization process, leading finally to large single crystals. Procedure B yields a large number of polycrystalline ZSM-5 aggregates through a mechanism which involves a preliminary formation and stabilization of very small X-ray amorphous zeolite particles. Operating conditions were described previously (*12, 13*). In both cases, the gel mixture was divided into several portions and sealed in identical 15-ml Pyrex tubes prior to autoclaving. They

0021-9517/83 $3.00

were heated under autogenous pressure, with occasional shaking, for given periods of time and progressively removed in order to isolate materials with increasing degree of crystallinity. After cooling, each sample (gel + zeolite) was filtered, washed abundantly with cold water and dried for 12 h at 120°C. The percentage of ZSM-5 in the as-crystallized phases was evaluated by both X-ray diffraction (XRD) and DTA techniques described previously (*12, 14*). Their global Si and Al content was determined by proton-induced γ-ray emission (*20*).

The HRMAS ^{13}C-NMR spectra of the solid intermediate phases were recorded at room temperature using the cross-polarization technique, on a Bruker CXP-200 high power NMR spectrometer, operating in the Fourier transform mode. A single contact sequence with a contact time of 6 ms using 8K data points and a sweep width of 10 kHz were used. The ^{13}C (50.3 MHz) and ^{1}H (200.0 MHz) rf-fields were of 46.7 G and 11.7 G, respectively. Magic angle spinning was at 3.1 kHz with a perdeuderated polymethylmethacrylate rotor. Two thousand FID's were accumulated before Fourier transformations. The total intensities were computed from the surface areas of the lines corresponding to the three carbon atoms of the propyl chains belonging to TPA entities.

Figure 1 illustrates the changes in relative ^{13}C-NMR intensities, linewidths and chemical shifts that occur when TPA ions begin to interact strongly and specifically with the different environments of the zeolite lattice (*18*). In particular, occluded TPA species (spectra B and C) give different ^{13}C-NMR spectra from the "free" TPA^+ ions of a solid ionic TPABr lattice (spectrum A). A complete variation of the C_1, C_2, and C_3 linewidths and total intensities, as a function of the synthesis time, for both procedures A and B, is compared in Table 1 and illustrated in Fig. 2.

In synthesis A, a limited number of ZSM-5 nuclei is formed at the expense of the amorphous Al-rich gel phase. They grow

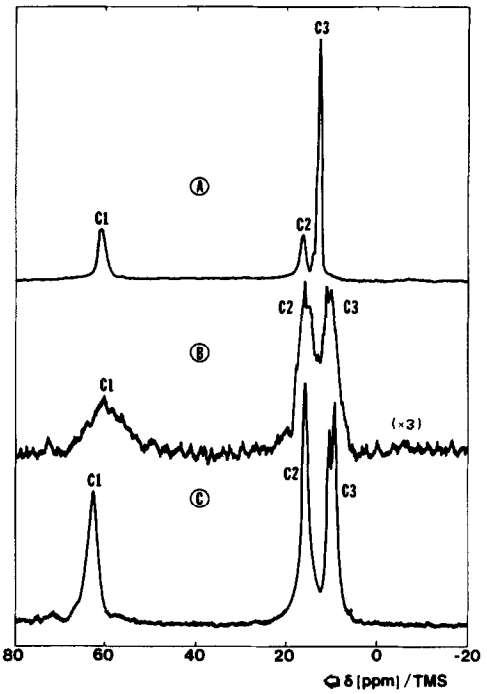

FIG. 1. HRMAS-^{13}C-NMR spectra of solid TPABr (A), TPA^+ occluded in sample B (20 h) (B) and in sample B (110 h) (C). NMR lines are assigned to carbon atoms of the propyl chains in $^{+}N(\overset{1}{C}H_2—\overset{2}{C}H_2—\overset{3}{C}H_3)_4$, as indicated.

slowly through a liquid phase ion transportation mechanism, by progressively incorporating the TPA species which were

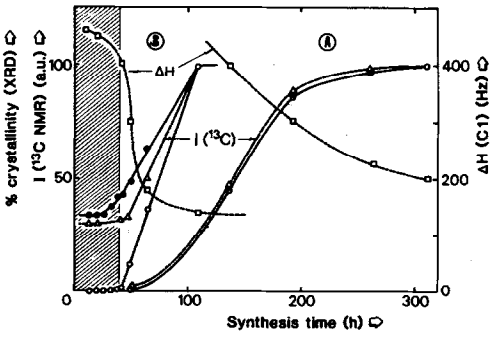

FIG. 2. Variation of ^{13}C-NMR parameters (Δ = total intensity, $\square$ = C1 linewidth, ΔH) and the percentage of crystallinity ($\circ$ = from XRD, $\bullet$ = from DTA) of various A and B intermediate phases, as a function of synthesis time.

TABLE 1

Variation of ^{13}C-NMR Parameters Characterizing Occluded $^{+}N(\overset{1}{C}H_2—\overset{2}{C}H_2—\overset{3}{C}H_3)_4$ Species in ZSM-5 Crystallites, with Percentage of Crystallinity, for Various A- and B-Type Intermediate Phases

Synthesis		Si/Al atomic ratio	% Crystallinity[a]		HRMAS-^{13}C-NMR parameters			
Type	Time (h)		XRD	DTA	Total intensity[a] (a.u.)	Linewidth (Hz) C1	C2	C3
A	48	1.8	0	0	0	—	—	—
	136	5.0	45	50	46	400	180	190
	192	10.0	86	92	87	300	140	140
	264	12.1	96	—	97	230	130	120
	312	13.2	100	100	100	200	130	120
B	14	33.6	0	34	30	450	200	200
	20	32.0	0	34	30	440	170	190
	26	34.2	0	34	—	—	—	—
	32	34.1	0	38	—	—	—	—
	38	34.3	0	42	—	—	—	—
	42	36.3	0	43	32	400	—	—
	49	36.3	12	49	32	300	130	120
	64	32.0	38	63	50	180	110	130
	110	36.1	100	100	100	140	80	120
	250	34.0	100	100	100	135	90	120
Solid Br $N(CH_2—CH_2—CH_3)_4$						80	85	30

[a] Sample B (110 h) proved to be 100% crystalline ZSM-5 as referred to a standard 100% crystalline ZSM-5 material (*12*), while sample A (312 h) was about 92% crystalline ZSM-5, according to the same standard. For the sake of simplicity, for each type of preparation, the ^{13}C-NMR intensities and crystallinities were normalized to 100 for the corresponding end phase.

shown to act as templates all along the growth process (*12*). As a result, the TPA content of an intermediate solid phase is directly proportional to its XRD crystallinity. No ^{13}C-NMR signal is detected at zero crystallinity (sample A, 48 h), confirming the absence of framework occluded TPA. The eventual excess of TPA impregnating the gel was completely eliminated by washing. As the crystallization proceeds, more and more TPA is progressively and regularly incorporated within the zeolite framework which is formed. The ^{13}C-NMR intensity, if normalized to 100 for a 100% crystalline material, will then be directly proportional to the XRD or DTA crystallinity (Fig. 2).

Conversely, in synthesis B, the hydrogel which is initially formed has a composition not too different from that expected from the ratio of the reagents (*12*). Its nucleation occurs rapidly and a large number of nuclei is formed, due to the high concentration of reactive aluminate and silicate species which are in intimate interaction with TPA structure-directing cations. They rapidly yield by hydrogel phase transformation a large number of ZSM-5 crystallites which are too small to be detected by XRD. However, these strongly bound TPA species can already be detected by DTA or ^{13}C-NMR. The phase isolated from the B-type synthesis appears to be already 30–35% crystalline after only 14 h autoclaving. After 49 h in the autoclave the size of the crystallites begins to be detectable by XRD and both "NMR and XRD crystallinities" then increase in a parallel way, illustrating again

that the template TPA species are progressively entrapped within the growing crystallites. It was in fact confirmed that 100% crystalline ZSM-5 obtained either from synthesis A or B has its entire pore volume filled with TPA entities (*18*).

Similarly, for both syntheses A and B, the linewidth of carbon atom C1, chosen as example, becomes narrower as the crystallization proceeds. The presence of the ^{14}N quadrupolar nucleus in the TPABr molecule has a definite effect on the linewidths and intensities even in the crystalline phase (*18*). In addition, the distribution of chemical shifts and a higher electric field gradient due to the less symmetric environment, do increase the linewidth. The influence of these latter effects enables one to relate the change in ΔH to crystallinity. The narrowing of ΔH reflects the progressive reorganization of the Si–Al framework around the propyl chains. In the early stages of the nucleation, some TPA units, only partially incorporated into the crystalline framework, could interact with heterogeneous environments of the surrounding gel phase, leading therefore to a broadening of the ^{13}C-NMR lines. In addition, NMR lines are narrower for sample B (110 h) than for sample A (312 h), confirming the lower absolute crystallinity of the latter (see the footnote to Table 1).

It is concluded that ^{13}C-NMR can be considered, along with DTA, as a very accurate technique for yielding valuable information on the nucleation and crystal growth processes of ZSM-5 type zeolites and, in particular, to evaluate the actual crystallinity of an intermediate phase. While XRD only reflects the progressive growth of the crystallites, ^{13}C-NMR gives additional information on slight transformations and reorganizations that already occur during the early nucleation processes. It also detects the moment at which the actual growth starts, by showing a sharp increase in the variation of different parameters (cf. Table 1 and Fig. 2). As a result, the actual synthesis time range where very small XRD amorphous ZSM-5 crystallites are formed and stabilized can be easily delineated (see synthesis B, hatched domain in Fig. 2).

Recent investigations have shown that the variation of ^{27}Al- and ^{29}Si-NMR parameters obtained by the high resolution solid state magic-angle-spinning technique are also very sensitive to the progressive ordering of the Si–Al framework during the growth process of ZSM-5 crystallites, and could be successfully used as a valuable complementary method (*15*).

ACKNOWLEDGMENTS

The authors thank Mr. G. Daelen for his skillful help in obtaining the CP/MAS ^{13}C-NMR spectra.

REFERENCES

1. Weisz, P. B., *Pure Appl. Chem.* **52,** 2091 (1980) and references therein.
2. Derouane, E. G., *in* "Catalysis by Zeolites" (B. Imelik *et al.*, Eds.), p. 5. Elsevier, Amsterdam, 1980, and references therein.
3. Derouane, E. G., and Gabelica, Z., *J. Catal.* **65,** 486 (1980).
4. Védrine, J. C., Auroux, A., Dejaifve, P., Ducarme, V., Hoser, H., and Zhou, S. B., *J. Catal.* **73,** 147 (1982).
5. Derouane, E. G., Dejaifve, P., Gabelica, Z., and Védrine, J. C., *Faraday Discuss. Chem. Soc.* **72,** 331 (1981).
6. Kaeding, W. W., Chu, C., Young, L. B., Weinstein, B., and Butter, S. T., *J. Catal.* **67,** 159 (1981).
7. Gabelica, Z., Gilson, J. P., and Derouane, E. G., *in* "Proceedings, 2nd European Symposium of Thermal Analysis" (D. Dollimore, Ed.), p. 434. Heyden, London, 1981.
8. Gabelica, Z., Gilson, J. P., Debras, G., and Derouane, E. G., *in* "Proceedings, 7th International Conference Thermal Analysis" (B. Miller, Ed.), p. 1203. Wiley/Heyden, New York, 1982.
9. Dejaifve, P., Auroux, A., Gravelle, P. C., Védrine, J. C., Gabelica, Z., and Derouane, E. G., *J. Catal.* **70,** 123 (1981).
10. Haag, W. O., and Olson, D. H., U.S. Patent 4,117,026, assigned to Mobil Oil Corp., 1978.
11. Auroux, A., Dexpert, H., Leclercq, C., and Védrine, J. C., *Appl. Catal.* **6,** 95 (1983).
12. Derouane, E. G., Detremmerie, S., Gabelica, Z., and Blom, N., *Appl. Catal.* **1,** 201 (1981).
13. Gabelica, Z., Blom, N., and Derouane, E. G., *Appl. Catal.* **5,** 227 (1983).
14. Jacobs, P. A., Derouane, E. G., and Weitkamp, J., *J. Chem. Soc. Chem. Commun.* **1981,** 591.

15. Gabelica, Z., B. Nagy, J., Debras, G., and Derouane, E. G., *in* "Proceedings, 6th International Conference Zeolites," Reno, 1983, in press.
16. Coudurier, G., Naccache, C., and Védrine, J. C., *J. Chem. Soc. Chem. Commun.* **1982,** 1413.
17. Boxhoorn, G., Van Santen, R. A., Van Erp, W. A., Hays, G. R., Huis, R., and Clague, D. J., *Chem. Soc. Chem. Commun.* **1982,** 264.
18. B. Nagy, J., Gabelica, Z., and Derouane, E. G., *Zeolites* **3,** 43 (1983).
19. Gabelica, Z., Derouane, E. G., and Blom, N., *Appl. Catal.* **5,** 109 (1983).
20. Debras, G., Derouane, E. G., Gilson, J. P., Gabelica, Z., and Demortier, G., *Zeolites* **3,** 37 (1983).

ZELIMIR GABELICA
JANOS B. NAGY[1]
GUY DEBRAS

Laboratoire de Catalyse
Facultés Universitaires de Namur
Rue de Bruxelles, 61
B-5000 Namur
Belgium

Received February 17, 1983

[1] To whom all correspondence should be addressed.